Acta Biochim Biophys Sin 2022, 54(10): 1528–1539
https://doi.org/10.3724/abbs.2022138
Advance Access Publication Date: 14 October 2022
Original Article

Original Article

MCU knockdown in hippocampal neurons improves memory performance of an Alzheimer's disease mouse model

Hongyan Cai[1,2,3,†,*], Jing Qiao[1,†], Siru Chen[1], Junting Yang[4], Christian Hölscher[5], Zhaojun Wang[2,3,4], Jinshun Qi[2,3,4], and Meina Wu[2,3,4,*]

[1]Department of Microbiology and Immunology, Shanxi Medical University, Taiyuan 030001, China, [2]Key Laboratory of Cellular Physiology (Shanxi Medical University), Ministry of Education, Taiyuan 030001, China, [3]Key Laboratory of Cellular Physiology, Shanxi Province, China, [4]Department of Physiology, Shanxi Medical University, Taiyuan 030001, China, and [5]Academy of Chinese Medical Science, Henan University of Chinese Medicine, Zhengzhou 450046, China

[†]These authors contributed equally to this work.

*Correspondence address. Tel: +86-13754805080; E-mail: yancai1@163.com (H.C.) / Tel: +86-13834678553; E-mail: wmna@163.com (M.W.)

Received 26 January 2022 Accepted 18 April 2022

Abstract

Alzheimer's disease (AD) is a progressive and degenerative disorder accompanied by cognitive decline, which could be promoted by mitochondrial dysfunction induced by mitochondrial Ca^{2+} (mCa^{2+}) homeostasis Mitochondrial calcium uniporter (MCU), a key channel of mCa^{2+} uptake, may be a target for AD treatment. In the present study, we reveal for the first time that *MCU* knockdown in hippocampal neurons improves the memory performance of APP/PS1/tau mice through radial arm maze task. Western blot analysis, transmission electron microscopy (TEM), Golgi staining, immunohistochemistry (IHC) and ELISA results demonstrate that *MCU* knockdown in hippocampal neurons upregulates the levels of postsynaptic density protein 95 (PSD95) and synaptophysin (SYP), and increases the numbers of synapses and dendritic spines. Meanwhile, *MCU* knockdown in hippocampal neurons decreases the neuroinflammatory response induced by astrogliosis and high levels of IL-1β and TNF-α, and improves the PINK1-Parkin mitophagy signaling pathway and increases the level of Beclin-1 but decreases the level of P62. In addition, *MCU* knockdown in hippocampal neurons recovers the average volume and number of mitochondria. These data confirm that *MCU* knockdown in hippocampal neurons improves the memory performance of APP/PS1/tau mice through ameliorating the synapse structure and function, relieving the inflammation response and recovering mitophagy, indicating that MCU inhibition has the potential to be developed as a novel therapy for AD.

Key words Alzheimer's disease, mitochondrial calcium uniporter, memory behavior deficit, neuroinflammation response, mitophagy

Introduction

Alzheimer's disease (AD) is considered to be the most common progressive neurodegenerative disease and the leading cause of dementia, with gradual deterioration of cognitive ability in individuals [1]. It has been predicted that the number of AD patients will be more than 110 million by 2050 due to the increasing aging population worldwide [2]. Several treatment strategies for AD have failed or are forced to stop due to serious side effects [3]. Importantly, AD is difficult to diagnose at the early stage. Therefore, effective and early therapeutic intervention is essential to reduce or stop the progression of AD [4].

In recent years, mitochondrial dysfunction in AD patients has attracted increasing attention [5]. One study showed that female amyloid precursor protein (APP)/presenilin1 (PS1)/tau transgenic AD mice developed mitochondrial dysfunction at three months of age. Female APP/PS1/tau mice showed typical pathological features of AD, including amyloid plaques, tau tangle formation and degeneration of neurons at six months of age [6]. Based on

consistent evidence, the mitochondrial theory of AD put forward by scientists [7] is that mitochondrial dysfunction directly promotes the development of AD from an early age [8,9].

The imbalance of mitochondrial calcium (mCa^{2+}) homeostasis is an important cause of mitochondrial dysfunction [10,11]. The mCa^{2+} uniporter (MCU) complex, localized in the inner mitochondrial membrane (IMM), is a key channel of mCa^{2+} uptake and is widely expressed in different cell types, including neurons [12]. MCU is the pore-forming homo-oligomer subunit, and loss of this subunit results in complete loss of MCU complex function [13,14]. Harrington *et al*. [15] first created *MCU*-KO mice and confirmed that in contrast to control (C57) mice, the mitochondrial uptake of Ca^{2+} in *MCU*-KO mice was significantly reduced [15]. In contrast, high expression of MCU, which was observed in the hippocampus of APP/PS1/tau mice in our experiment, could induce high mCa^{2+} uptake, ultimately leading to mitochondrial dysfunction [15]. Therefore, MCU might play an important role in the development of AD [16].

In the present study, we investigated the therapeutic potential of *MCU* knockdown in hippocampal neurons in APP/PS1/tau mice and explored the possible mechanisms by which *MCU* knockdown ameliorates neuronal function and memory formation.

Materials and Methods

Animals

A total of 63 amyloid precursor protein (APP)/presenilin1 (PS1)/tau female mice (eight months old) containing three gene mutations (PS1M146V, APPSwe and tauP301L), were obtained from Jackson Laboratory (Bar Harbor, USA). Totally, 21 wild-type (WT) female mice (eight months old) with the same genetic background (C57BL/6J) purchased from the Animal Research Center of Shanxi Medical University were used as control mice. Compared with APP/PS1/tau male mice, female mice showed more progressed pathological characteristics in the brain and cognitive behavior impairments. Therefore, to reduce the difference caused by sex on pathological characteristics and cognitive behavior, APP/PS1/tau female mice were selected in our study. Mice were kept in an independent air supply system with a 12 h/12 h light-dark cycle at 23 ± 2°C and 55% ± 5% humidity and supplied with standard food and water. All animal experimental procedures were approved by the Institutional Animal Care Committee of Shanxi Medical University.

Injection of adeno-associated virus (AAV)-9 containing a neuron-specific promoter hsyn in the hippocampus

AAV-9 (1×10^{12} μg/mL) containing hsyn, coating Control-shRNA and MCU-shRNA (Hanheng Biotechnology Co., Ltd, Shanghai, China) were employed. Sequence of Control-shRNA (shCon) is: 5′-GATCCGTTCTCCGAACGTGTCACGTAATTCAAGAGATTACGTGACACGTTCGGAGAATTTTTTC-3′ (sense), 3′-AATTGAAAAAATTCTCCGAACGTGTCACGTAATCTCTTGAATTACGTGACACGTTCGGAGAACG-5′ (antisense); and sequence of MCU-shRNA (shMCU) is: 5′-GATCCGTAACATACCACGTACGGCCACCAAATTCAAGAGATTTGGTGGCCGTACGTGGTATGTTATTTTTTG-3′ (sense), and 3′-AATTCAAAAAATAACATACCACGTACGGCCACCAAATCTCTTGAATTTGGTGGCCGTACGTGGTATGTTACG-5′ (antisense).

Mice were divided into 4 groups (21 mice in each group): WT, APP/PS1/tau, APP/PS1/tau + shCon and APP/PS1/tau + shMCU. Two groups (WT + shCon and WT + shMCU) were not included in this study because we mainly focused on the effect of shCon or shMCU on APP/PS1/tau mice, according to the purpose of this study. Mice were anesthetized with isoflurane, and their heads were fixed with ear bars in the brain stereotactic apparatus (Robot Stereotaxic Serial; Neurostar, Tübingen, Germany). The temperature of the mice was maintained by a heating pad during the whole operation, and eye ointment was applied to the eyes to avoid dryness. Hair was shaved from the surgical area and disinfected with iodophor, and then the skin was cut along the middle of the cranial crest. The skull surface was cleaned with 10% H_2O_2 to expose the anterior fontanel and posterior fontanel of the skull. Two microliters of shMCU or shCon was injected into the hippocampus of each mouse according to the atlas of the mouse brain [–1.6 mm anteroposterior (AP), ± 1.8 mm mediolateral (ML), –1.6 mm dorsoventral (DV)] at a rate of 0.2 μL/min using a 5-μL Hamilton syringe connected to a 30-gauge needle [17]. After injection, low viscosity silica gel was used to cover the skull surface and sutured wound skin. Mice were placed on a 37°C thermal pad for observation until they woke up without obvious abnormal activity. Then, the mice were returned to their home cages while kept warm. After a 4-week period of recovery, western blot analysis (4 groups with 3 mice in each group) was used to observe the effect of virus transfection *in vivo*. Other mice (4 groups with 18 mice in each group) were used for the behavioral experiment and subsequent analyses.

Radial arm maze task

The radial arm maze task was performed to test the working memory and reference memory of rodents as described previously [18]. The radial maze (SMART; Panlab Harward Apparatus, Bioscience Company, Holliston, USA) consists of 8 arms (30 cm in length, 15 cm in width and 7 cm in height), starting from a central octagonal area (32 cm in diameter). At the end of each arm, there is a food cup. Several extra maze cues were placed on the walls around the maze. Mice were housed individually and were food-restricted to 80%–85% of their free-feeding weights, with freely available water. In the training test, 30 mg food pellets were placed at the end of each arm. Mice were placed in the center of the maze and allowed to explore freely until either 10 min elapsed or food pellets were eaten. Following the 5-day training period, each mouse was placed in the center of the maze and subject to working memory tests and reference memory tests for 10 days. During the test period, only the food cups of four arms (numbered 1, 2, 4 and 7) were filled with food pellets. The four arms were configured so that two of these arms were adjacent, and the other arms were 90° apart. The trial commenced with the placement of each mouse on the central platform and finished when the food pellets were consumed or until 10 min elapsed, whichever occurred first. At the end of each trial, the maze was cleaned with 75% ethanol. The number of arm entries was recorded. Re-entry into baited arms was regarded as working memory errors (WMEs), while the number of entries into unbaited arms was regarded as reference memory errors (RMEs).

Western blot analysis

The hippocampi of mice were dissected, and protein was extracted using the tissue protein extraction reagent (Boster, Wuhan, China) following the instructions of the manufacturer; complete protease inhibitor was added to hippocampal tissue at a ratio of 1:10 by weight (Boster). Protein concentration was measured using a bicinchoninic acid protein assay kit (Boster) after removing tissue fragments by low-speed centrifugation. Protein samples were

separated on a 12% sodium dodecyl sulfate (SDS)-polyacrylamide gel. After electrophoresis, the proteins were transferred onto PVDF membranes, and nonspecific binding was blocked with 5% bovine serum albumin (BSA) in Tris-buffered saline with 0.05% Tween-20 (TBST). Membranes were incubated overnight with primary antibodies at 4°C, followed by incubation with the corresponding secondary antibodies at room temperature for 2 h. The following primary antibodies (all from Abcam, Cambridge, UK) were used: anti-GAPDH (ab226408; 1:5000), anti-β-actin (ab8226, 1:5000), anti-MCU (ab219827, 1:1000), anti-PSD95 (ab76115, 1:1000), anti-SYP (ab52636, 1:3000), anti-PINK1 (ab23707, 1:1000), anti-Parkin (ab77924, 1:2000), anti-Beclin-1 (ab207612, 1:2000), and anti-P62 (ab109012, 1:1000). The secondary antibodies were anti-rabbit IgG-HRP conjugate (BA1054, 1:5000; Boster) and anti-mouse IgG-HRP conjugate (BA1050, 1:5000; Boster). Immunocomplexes were visualized using an enhanced chemiluminescence detection kit (Beyotime, Shanghai, China). Signals on membranes were scanned with a FluorChem scanner (Protein Simple; Bio-Techne, Minneapolis, USA) and quantified with Alpha View SA software (Azure C300 Biosystems; Azure Biosystems, Dublin, USA).

Transmission electron microscopy (TEM)

Mice were anesthetized with isoflurane. The chest cavities were opened, and the animals were cardio-perfused with 4% paraformaldehyde (PFA). The hippocampi were removed, cut into 1 mm^3 pieces and fixed in glutaric acid at room temperature for 2 h at 4°C overnight. Tissues were washed with 0.1 M phosphate buffered saline (PBS) 3 times and fixed with 1% osmium acid at room temperature for 3 h. Tissue samples were placed in 50%, 70% and 90% alcohol baths for gradient alcohol dehydration, followed by gradient acetone dehydration in an alcohol-acetone mixture (ratio of 90% acetone and 90% alcohol was 1:1), 90% and 100% acetone. Tissue samples were incubated with embedding agent/acetone (1:2) at room temperature for 4 h, embedding agent/acetone (2:1) at room temperature overnight, and embedding agent at 37°C for 3 h. Tissues were embedded in the oven at 37°C overnight, at 45°C for 12 h, and at 60°C for 48 h. Tissues were cut into 60–80 nm sections. Sections were stained with uranium dioxide acetate for 30 min, washed with distilled water 3 times, stained with lead citrate for 10 min, washed with distilled water 3 times, and dried at room temperature overnight. A transmission electron microscope (JEM-1011; JEOL, Tokyo, Japan) was used to observe synapses and mitochondria. Image J software (NIH, Bethesda, USA) was used to mark and count the numbers of synapses and the average volume and numbers of mitochondria.

Immunohistochemistry (IHC)

Mice were sacrificed by cardiac perfusion-fixation with PBS and 4% PFA. Brains were fixed in 4% PFA for 24 h and incubated in 30% sucrose at room temperature for 24 h. Brains were embedded in OCT frozen embedding medium (Leica Biosystems, Wetzlar, Germany). Coronal sections were cut at 25 μm on a freezing microtome (CM1850; Leica Biosystems) and stored in PBS at 4°C. Sections were incubated with 5% hydrogen peroxide at room temperature for 15 min and blocked with 5% goat serum (Solarbio, Beijing, China) for 30 min. Afterwards, sections were incubated with the anti-GFAP primary antibody (bs-0199R, 1:200; Bioss, Beijing, China) at 4°C overnight, followed by treatment with the peroxidase-conjugated Affinipure goat anti-rabbit IgG(H + L) secondary antibody (1:200; ZSGB-BIO, Beijing, China) at 37°C for 2 h. The glial fibrillary acidic protein (GFAP) area was observed with a BX51 microscope (Olympus, Tokyo, Japan) and measured using Image-Pro Plus 6.0 (Media Cybernetics, Rockville, USA).

Enzyme-linked immunosorbent assay (ELISA)

ELISA was carried out to measure the levels of IL-1β and TNF-α using the corresponding kits (Xitang, Shanghai, China) according to the manufacturer's instructions. Samples were added into 96-well plates and incubated at 37°C for 2 h. Test solution A (biotinylated antibody working solution) was added, and the plate was covered with a film and incubated at 37°C for 1 h. The liquid in each well was discarded and washed 3 times. Detection solution B (HRP enzyme binder working solution) was added, and the plate was covered with a film and incubated at 37°C for 30 min. The liquid in each sample well was discarded and the wells were washed 5 times, and substrate solution was added to each well and incubated in the dark at 37°C for 20 min. After addition of the stop solution, the optical density (OD) value of each well was measured at 450 nm with a microplate reader. The levels of IL-1β and TNF-α were calculated using the standard curves.

Golgi staining

Brains were put into Golgi immersion solution (Solution A containing potassium dichromate and mercuric chloride: Solution B containing potassium chromate = 1:1) at room temperature in the dark for 14 days, with the immersion solution changed each day. After two weeks, the brains were put into Solution C for 5 days, with the solution refreshed each day. Brains were placed on sample platforms and quickly frozen on dry ice for 10 min. Samples were cut into 100-μm-thick sections with a frozen section microtome (CM1520; Leica Biosystems), which were suitable for pathological and biological examination Sections were mounted on gelatinated slides and dried in the dark. Sections were washed with distilled water, stained with dye for 10 min, and washed again. The stained sections were dehydrated in 50%, 75% and 95% ethanol for 4 min and then dehydrated in anhydrous ethanol 4 times. Sections were washed with xylene 3 times and sealed with resin [19]. Dendritic spines were observed with a Digital Tissue Slice Scanning System (Aperio, San Diego, USA). Dendritic spines were manually marked and total numbers of dendritic spines were calculated using Image J software (NIH, Bethesda, USA) [19].

Statistical analysis

All data are expressed as the mean ± SEM. All statistical analyses were performed with SPSS 13.0 and SigmaPlot 12.3 software. Statistical comparison was performed by using one-way analysis of variance (ANOVA), followed by Tukey's test. Differences between groups were considered statistically significant at $P < 0.05$.

Results

Successful knockdown of *MCU* in hippocampal neurons

In order to confirm the successful knockdown of *MCU* in the hippocampal neurons of APP/PS1/tau mice, we measured the expression level of MCU by western blot analysis. As shown in Figure 1A,B, the relative expression level of MCU in the hippocampus was significantly higher ($P < 0.01$) in the APP/PS1/tau group (1.92 ± 0.13) compared with that in the WT group (1.00 ± 0.12). The expression level of MCU in the hippocampus was lower

in the APP/PS1/tau + shMCU group (1.34 ± 0.08) than in the APP/PS1/tau group (1.92 ± 0.13, $P < 0.05$) or the APP/PS1/tau + shCon group (1.96 ± 0.09, $P < 0.05$). There was no significant difference between the APP/PS1/tau group and the APP/PS1/tau + shCon group ($P > 0.05$). These data indicated that AAV-9, containing hsyn, coated with shMCU or shCon, successfully infected hippocampal neurons and effectively interfered with the expression of MCU in hippocampal neurons of APP/PS1/tau mice.

MCU knockdown in hippocampal neurons attenuated memory performance impairment in APP/PS1/tau mice

In order to observe whether *MCU* knockdown in hippocampal neurons could attenuate memory performance impairment in APP/PS1/tau mice, we tested the working memory and reference memory of mice (Figure 1C). As shown in Figure 1D, the APP/PS1/tau group had significantly more working memory errors (3.16 ± 0.26, $P < 0.001$) than the WT group (1.80 ± 0.14). However,

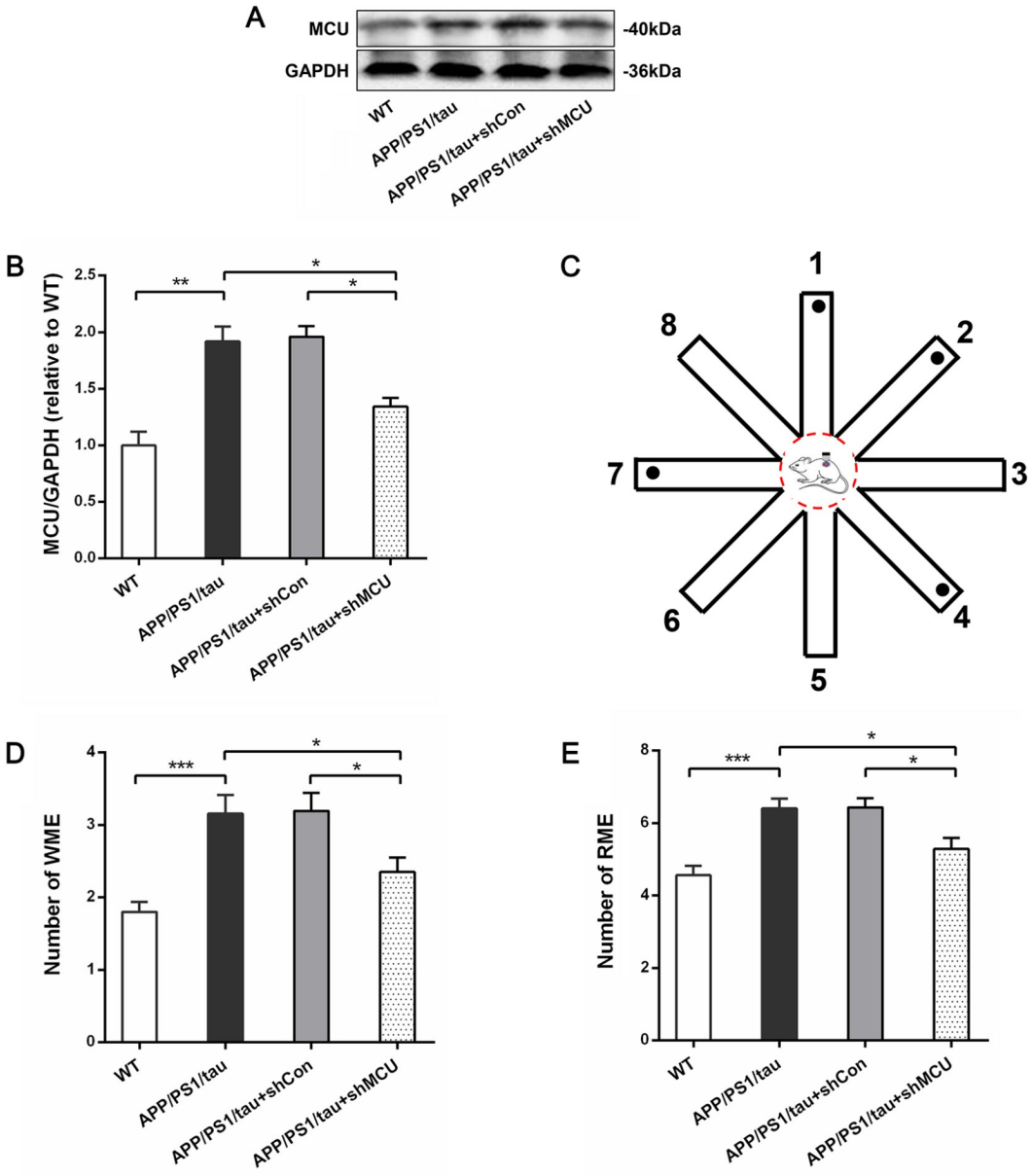

Figure 1. Successful establishment of APP/PS1/tau mice with *MCU* knockdown in hippocampal neurons and *MCU* knockdown in hippocampal neurons attenuated memory performance impairment of APP/PS1/tau mice (A) Representative western blots of the expression levels of MCU in the hippocampi of WT mice, APP/PS1/tau mice, APP/PS1/tau + shCon mice and APP/PS1/tau + shMCU mice. (B) Histograms showed that the expression level of MCU in the hippocampus of APP/PS1/tau mice was higher than that of WT mice and comparable to that of APP/PS1/tau mice or APP/PS1/tau + shCon mice. The expression level of MCU in the hippocampus was decreased in APP/PS1/tau + shMCU mice, showing that AAV-9, containing hsyn, coated with shMCU, successfully interfered with the expression of MCU in hippocampal neurons of APP/PS1/tau mice. $n = 3$ for each group. $^*P < 0.05$, $^{**}P < 0.01$. (C) A diagram showing the radial arm maze with reward locations (tiny black dots) at the end of four arms (1, 2, 4 and 7). Histograms showed that APP/PS1/tau mice had more working memory errors (D) and reference memory errors (E) than the WT mice; *MCU* knockdown in hippocampal neurons decreased the number of memory errors compared with APP/PS1/tau mice or APP/PS1/tau + shCon mice. $n = 18$ for each group. $^*P < 0.05$, $^{***}P < 0.001$.

error numbers were decreased in the APP/PS1/tau + shMCU group (2.36 ± 0.19), compared with the APP/PS1/tau group (3.16 ± 0.26, $P < 0.05$) or the APP/PS1/tau + shCon group (3.19 ± 0.25, $P < 0.05$). There was no difference between the APP/PS1/tau group and the APP/PS1/tau + shCon group ($P > 0.05$). Figure 1E showed that the APP/PS1/tau group had significantly more reference memory errors (6.41 ± 0.26, $P < 0.001$) than the WT group (4.56 ± 0.27). Error number was decreased in the APP/PS1/tau + shMCU group (5.29 ± 0.309) compared to that in the APP/PS1/tau group (6.41 ± 0.26, $P < 0.05$) or the APP/PS1/tau + shCon group (6.43 ± 0.26, $P < 0.05$), while no difference was found in the error numbers between the APP/PS1/tau group and the APP/PS1/tau + shCon group ($P > 0.05$). These findings indicated that *MCU* knockdown in hippocampal neurons effectively improved the working memory and reference memory of APP/PS1/tau mice.

MCU knockdown in hippocampal neurons increased the levels of PSD95 and SYP in APP/PS1/tau mice

In order to observe whether *MCU* knockdown in hippocampal neurons could enhance the synaptic function, we tested the levels of synaptic proteins PSD95 and SYP by western blot analysis. As shown in Figure 2A,B, compared to that in the WT group (1.00 ± 0.06), the relative level of PSD95 was significantly lower in the APP/PS1/tau group (0.61 ± 0.03, $P < 0.01$). The level of PSD95 was increased in the APP/PS1/tau + shMCU group (0.89 ± 0.03) compared with that in the APP/PS1/tau group (0.61 ± 0.03, $P < 0.05$) or the APP/PS1/tau + shCon group (0.63 ± 0.06, $P < 0.05$). There was no difference between the APP/PS1/tau group and the APP/PS1/tau + shCon group ($P > 0.05$). As shown in Figure 2A,C, compared to the WT group (1.00 ± 0.06), the relative level of SYP was significantly lower in the APP/PS1/tau group (0.64 ± 0.03, $P < 0.01$). However, the level of SYP was increased in the APP/PS1/tau + shMCU group (0.87 ± 0.06) compared with that in the APP/PS1/tau group (0.64 ± 0.03, $P < 0.05$) or the APP/PS1/tau + shCon group (0.61 ± 0.03, $P < 0.05$). There was no difference between the APP/PS1/tau group and the APP/PS1/tau + shCon group ($P > 0.05$). These data indicated that *MCU* knockdown in hippocampal neurons could enhance the synaptic function of APP/PS1/tau mice.

MCU knockdown in hippocampal neurons increased the numbers of synapses and dendritic spines

In order to observe whether *MCU* knockdown in hippocampal neurons could improve the synaptic structure, we measured the numbers of synapses and dendritic spines. As shown in Figure 2D,E, compared to that in the WT group (1.71 ± 0.08), synapse number was significantly lower in the APP/PS1/tau group (0.85 ± 0.05, $P < 0.001$). However, synapse number was increased in the APP/PS1/tau + shMCU group (1.13 ± 0.07) compared with that in the APP/PS1/tau group (0.85 ± 0.05, $P < 0.05$) or the APP/PS1/tau + shCon group (0.84 ± 0.05, $P < 0.05$). There was no difference between the APP/PS1/tau group and the APP/PS1/tau + shCon group ($P > 0.05$). As shown in Figure 2F,G, compared to that in the WT group (13.33 ± 70.6), dendritic spine number in the APP/PS1/tau group was significantly lower (8.17 ± 0.54, $P < 0.001$). Dendritic spine number was increased in the APP/PS1/tau + shMCU group (11.00 ± 0.58) compared with that in the APP/PS1/tau group (8.17 ± 0.54, $P < 0.05$) or the APP/PS1/tau + shCon group (8.50 ± 0.56, $P < 0.05$). There was no difference between the APP/PS1/tau group and the APP/PS1/tau + shCon group ($P > 0.05$). These data indicated that *MCU* knockdown in hippocampal neurons could improve the synaptic structure of APP/PS1/tau mice.

MCU knockdown in hippocampal neurons alleviated the activation of astrocytes and decreased the levels of IL-1β and TNF-α

In order to observe whether *MCU* knockdown in hippocampal neurons could alleviate the inflammatory response, we tested the activation of astrocytes and measured the levels of IL-1β and TNF-α by ELISA. Figure 3A,B showed that the percentage area of glial fibrillary acidic protein (GFAP) was significantly higher in the APP/PS1/tau group (21.77% ± 0.97%, $P < 0.001$) than in the WT group (14.83% ± 0.92%). However, the percentage area of GFAP was decreased in the APP/PS1/tau + shMCU group (16.77% ± 0.95%) compared with that in the APP/PS1/tau group (21.77% ± 0.97%, $P < 0.01$) or the APP/PS1/tau + shCon group (20.92% ± 1.00%, $P < 0.05$). There was no difference between the APP/PS1/tau group and the APP/PS1/tau + shCon group ($P > 0.05$). As shown in Figure 3C, the level of IL-1β was significantly higher in the APP/PS1/tau group (98.01 ± 7.15, $P < 0.001$) than in the WT group (51.75 ± 2.94). However, the level of IL-1β was decreased in the APP/PS1/tau + shMCU group (70.59 ± 4.55) compared with that in the APP/PS1/tau group (98.01 ± 7.15, $P < 0.05$) or the APP/PS1/tau + shCon group (99.23 ± 6.48, $P < 0.01$). There was also no difference between the APP/PS1/tau group and the APP/PS1/tau + shCon group ($P > 0.05$). Figure 3D showed that the level of TNF-α was significantly higher in the APP/PS1/tau group (44.99 ± 3.73, $P < 0.01$) than in the WT group (27.72 ± 1.49), while the level of TNF-α was decreased in the APP/PS1/tau + shMCU group (30.52 ± 2.55) compared to that in the APP/PS1/tau group (44.99 ± 3.73, $P < 0.05$) or the APP/PS1/tau + shCon group (43.68 ± 3.94, $P < 0.05$). There was no difference between the APP/PS1/tau group and the APP/PS1/tau + shCon group ($P > 0.05$). These data indicated that *MCU* knockdown in hippocampal neurons could alleviate the inflammatory response of APP/PS1/tau mice.

MCU knockdown in hippocampal neurons increased the levels of PINK1, Parkin and Beclin-1, decreased the level of P62, and recovered the average volume and number of mitochondria in APP/PS1/tau mice

In order to observe whether *MCU* knockdown in hippocampal neurons could upregulate the mitophagy pathway and improve the mitochondrial function, we assessed levels of PINK1, Parkin, Beclin-1, and P62, and the average volume and number of mitochondria. As shown in Figure 4A,B, compared to the WT group (1.00 ± 0.06), the relative level of PINK1 was significantly lower in the APP/PS1/tau group (0.57 ± 0.07, $P < 0.01$). The level of PINK1 was increased in the APP/PS1/tau + shMCU group (0.88 ± 0.06) compared with that in the APP/PS1/tau group (0.57 ± 0.07, $P < 0.05$) or the APP/PS1/tau + shCon group (0.51 ± 0.07, $P < 0.05$). There was no difference between the APP/PS1/tau group and the APP/PS1/tau + shCon group ($P > 0.05$). Figure 4A,C showed that compared to that in the WT group (1.00 ± 0.09), the level of Parkin was significantly lower in the APP/PS1/tau group (0.61 ± 0.03, $P < 0.01$). However, the level of Parkin was increased in the APP/PS1/tau + shMCU group (0.88 ± 0.048) compared with that in the APP/PS1/tau group (0.61 ± 0.03, $P < 0.05$) or the APP/PS1/tau + shCon group (0.60 ± 0.04, $P < 0.05$). There was also no difference

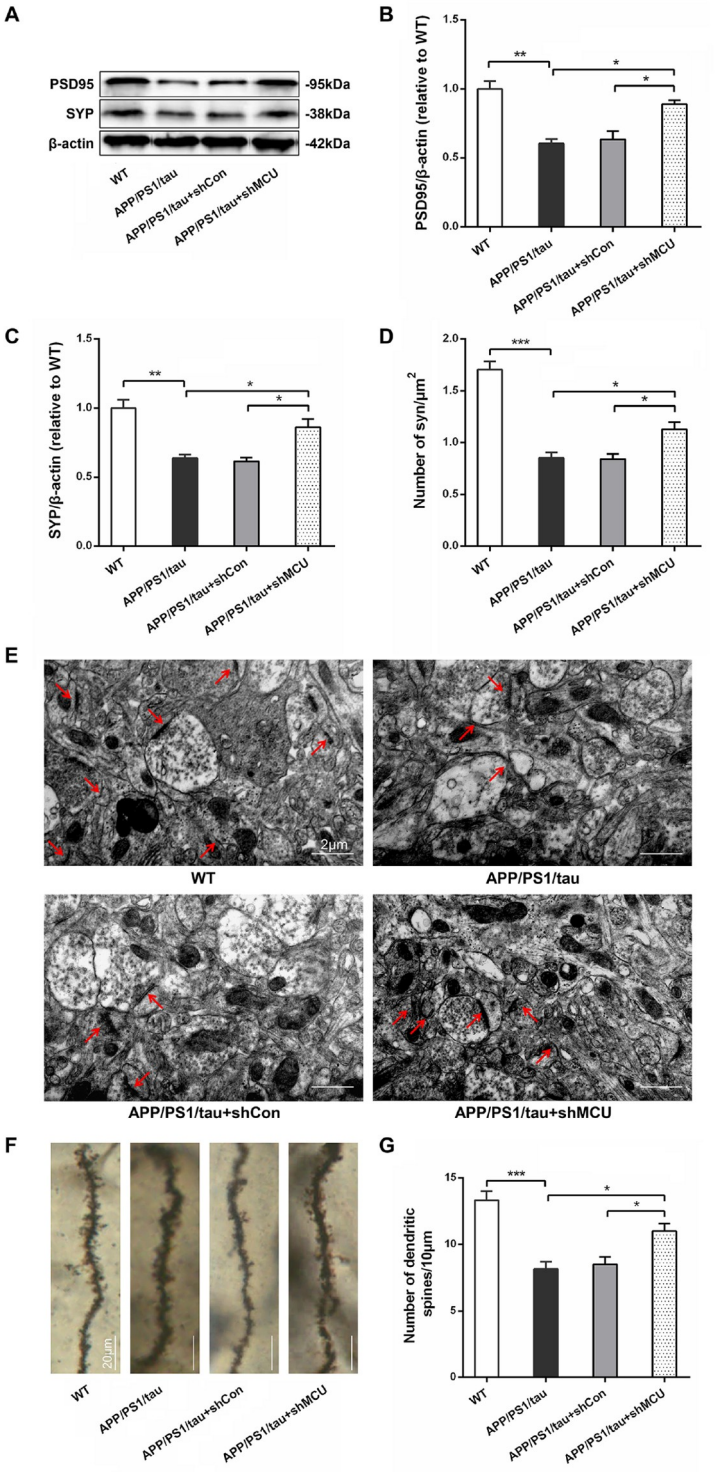

Figure 2. *MCU* knockdown in hippocampal neurons increased the levels of PSD95 and SYP and increased the numbers of synapses and dendritic spines in APP/PS1/tau mice (A) Representative western blots of the levels of PSD95, SYP and β-actin in the hippocampi of WT mice, APP/PS1/tau mice, APP/PS1/tau + shCon mice and APP/PS1/tau + shMCU mice. (B,C) The levels of PSD95 and SYP in APP/PS1/tau mice were lower than those in WT mice. The decrease in the levels of PSD95 and SYP in APP/PS1/tau mice or APP/PS1/tau + shCon mice was reversed by *MCU* knockdown in hippocampal neurons. $n = 3$ for each group. $^{*}P < 0.05$, $^{**}P < 0.01$. (D) Synapse number was lower in APP/PS1/tau mice than in WT mice; synapse number in APP/PS1/tau mice or APP/PS1/tau + shCon mice was improved by *MCU* knockdown in hippocampal neurons. (E) Typical electron micrographs of synapses are shown. The distribution of high electron density in synapses of the hippocampus was uneven, and the synaptic structure was abnormal in the APP/PS1/tau and APP/PS1/tau + shCon groups, which was reversed to some extent in the APP/PS1/tau + shMCU group. (F) Typical micrographs of dendritic spines. (G) Dendritic spine number was lower in APP/PS1/tau mice than in WT mice; dendritic spine number in APP/PS1/tau mice or APP/PS1/tau + shCon mice was improved by *MCU* knockdown in hippocampal neurons. $n = 6$ for each group. $^{*}P < 0.05$, $^{***}P < 0.001$.

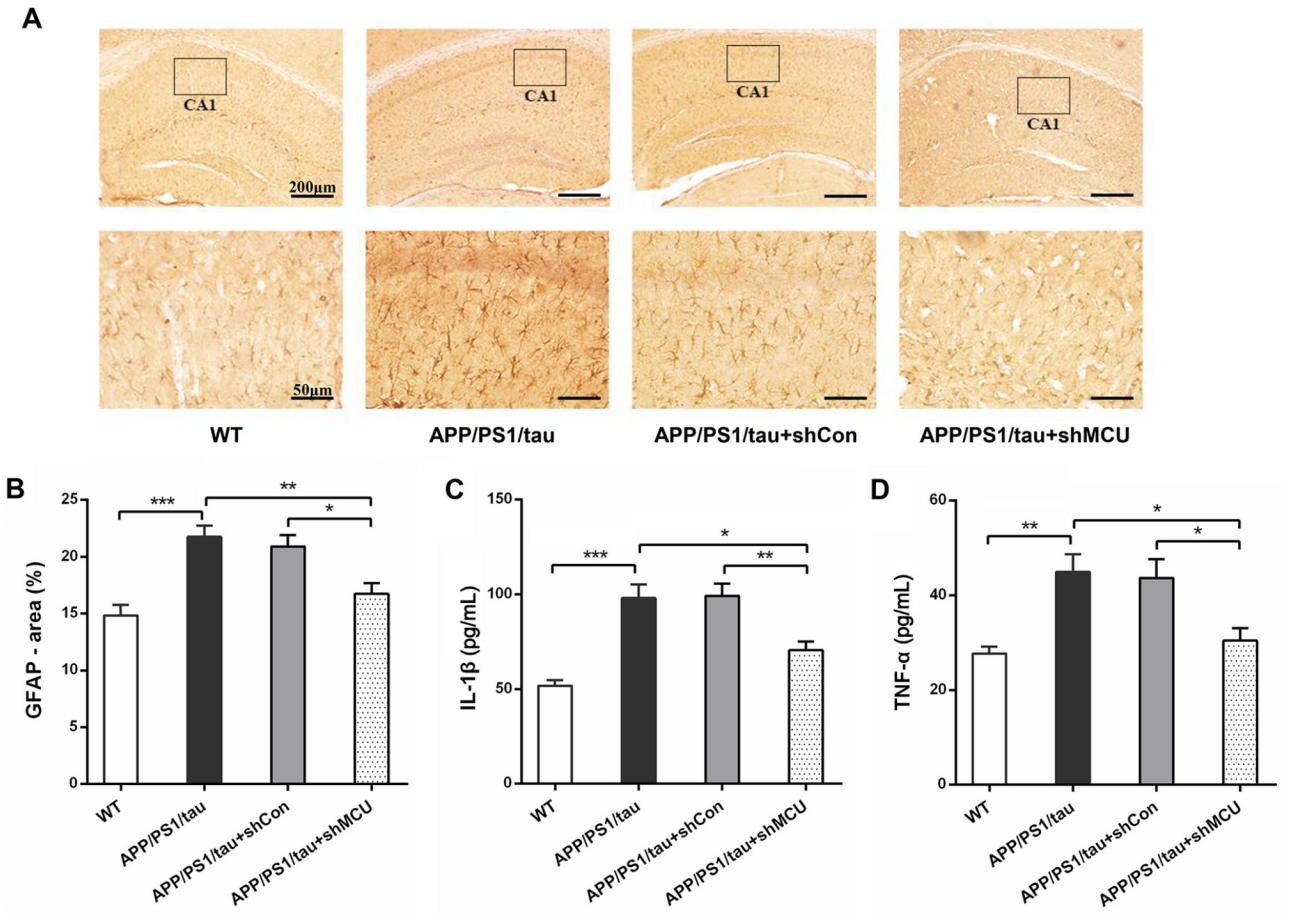

Figure 3. *MCU* knockdown in hippocampal neurons alleviated the stronger activation of astrocytes and decreased the levels of IL-1β and TNF-α in APP/PS1/tau mice (A) Representative immunohistochemical images of astrocyte activation in the hippocampi of WT mice, APP/PS1/tau mice, APP/PS1/tau + shCon mice and APP/PS1/tau + shMCU mice. (B) Histograms showing that the percentage area of GFAP in the hippocampus was higher in APP/PS1/tau mice than in WT mice. The increase in the percentage area of GFAP in APP/PS1/tau mice or APP/PS1/tau + shCon mice was reversed by *MCU* knockdown in hippocampal neurons. $n = 3$ for each group. $^{*}P < 0.05$, $^{**}P < 0.01$, $^{***}P < 0.001$. (C,D) Histograms showed that the levels of IL-1β and TNF-α in the hippocampus were higher in APP/PS1/tau mice than in WT mice; the levels of IL-1β and TNF-α in the hippocampus of APP/PS1/tau mice or APP/PS1/tau + shCon mice were decreased by *MCU* knockdown in hippocampal neurons. n = 6 for each group. $^{*}P < 0.05$, $^{**}P < 0.01$, $^{***}P < 0.001$.

between the APP/PS1/tau group and the APP/PS1/tau + shCon group ($P > 0.05$). As shown in Figure 4D,E, compared to that in the WT group (1.00 ± 0.03), the level of Beclin-1 was lower in the APP/PS1/tau group (0.82 ± 0.03, $P < 0.05$). However, the level of Beclin-1 was increased in the APP/PS1/tau + shMCU group (0.96 ± 0.03) compared with that in the APP/PS1/tau group (0.82 ± 0.03, $P < 0.05$) or the APP/PS1/tau + shCon group (0.82 ± 0.03, $P < 0.05$), while no difference was found between the APP/PS1/tau group and the APP/PS1/tau + shCon group ($P > 0.05$). As shown in Figure 4D,F, compared to that in the WT group (1.00 ± 0.05), the level of P62 was significantly higher in the APP/PS1/tau group (1.46 ± 0.05, $P < 0.01$). The level of P62 was decreased in the APP/PS1/tau + shMCU group (1.22 ± 0.05) compared with that in the APP/PS1/tau group (1.46 ± 0.05, $P < 0.05$) or the APP/PS1/tau + shCon group (1.47 ± 0.06, $P < 0.05$). There was no difference between the APP/PS1/tau group and the APP/PS1/tau + shCon group ($P > 0.05$).

As shown in Figure 4G,H, the average volume of mitochondria was smaller in the APP/PS1/tau group (0.115 ± 0.004, $P < 0.001$) than in the WT group (0.151 ± 0.004). However, the average volume of mitochondria was significantly increased in the APP/PS1/tau + shMCU group (0.141 ± 0.004) compared to that in the APP/PS1/tau group (0.115 ± 0.004, $P < 0.01$) or the APP/PS1/tau + shCon group (0.114 ± 0.005, $P < 0.01$). There was no difference between the APP/PS1/tau group and the APP/PS1/tau + shCon group ($P > 0.05$). As shown in Figure 4G,I, the number of mitochondria was significantly higher in the APP/PS1/tau group (1.20 ± 0.04, $P < 0.01$) than in the WT group (0.93 ± 0.05). Furthermore, the mitochondria number was decreased in the APP/PS1/tau + shMCU group (0.97 ± 0.06) compared with that in the APP/PS1/tau group (1.20 ± 0.04, $P < 0.05$) or the APP/PS1/tau + shCon group (1.18 ± 0.06, $P < 0.05$). There was no difference between the APP/PS1/tau group and the APP/PS1/tau + shCon group ($P > 0.05$). These data indicated that *MCU* knockdown in hippocampal neurons could upregulate the mitophagy pathway and improve the mitochondrial function of APP/PS1/tau mice.

Discussion

Evidence for calcium dysregulation in AD was initially found over 25 years ago in fibroblast cells isolated from AD patients [20]. The

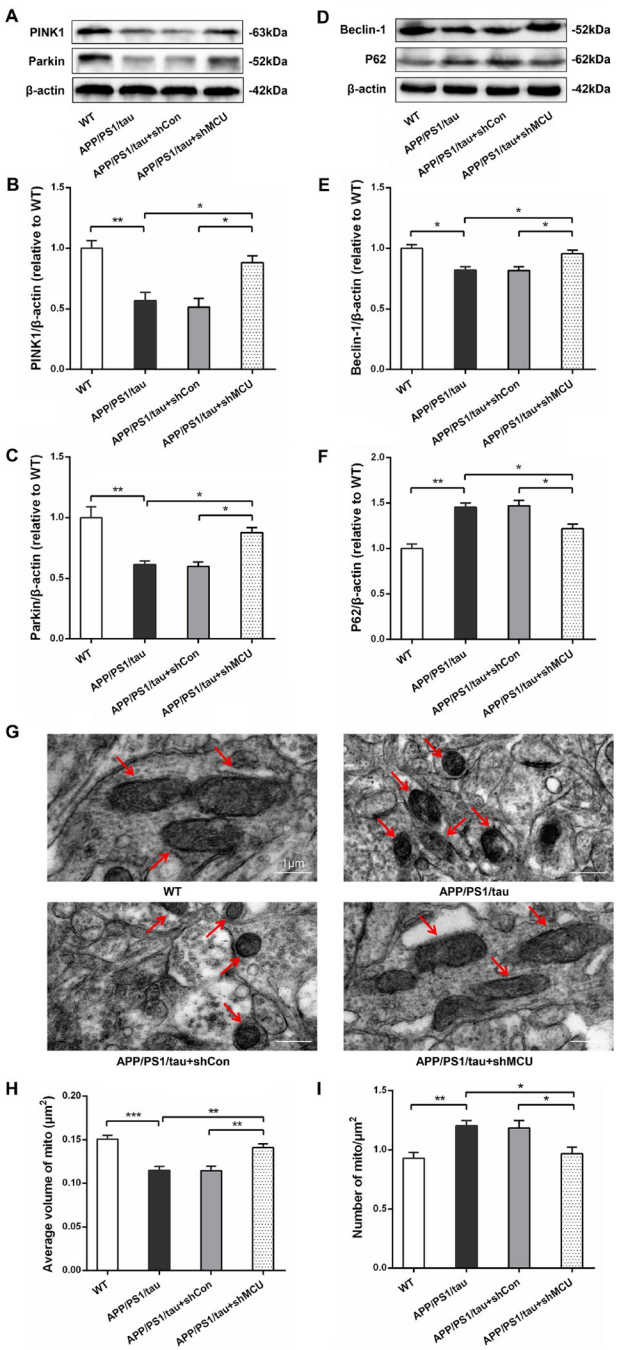

Figure 4. ***MCU* knockdown in hippocampal neurons increased the levels of PINK1, Parkin and Beclin-1, decreased the level of P62, and recovered the average volume and number of mitochondria in APP/PS1/tau mice** (A) Representative western blots of the levels of PINK1, Parkin and β-actin in the hippocampi of WT mice, APP/PS1/tau mice, APP/PS1/tau + shCon mice and APP/PS1/tau + shMCU mice. (B,C) The levels of PINK1 and Parkin in APP/PS1/tau mice were lower than those in WT mice. The decrease in the levels of PINK1 and Parkin in APP/PS1/tau mice or APP/PS1/tau + shCon mice was reversed by *MCU* knockdown in hippocampal neurons. $n = 3$ for each group. $^{*}P < 0.05$, $^{**}P < 0.01$. (D) Representative western blots of the levels of Beclin-1, P62 and β-actin in the hippocampi of WT mice, APP/PS1/tau mice, APP/PS1/tau + shCon mice and APP/PS1/tau + shMCU mice. (E,F) The level of Beclin-1 in APP/PS1/tau mice was lower than that in WT mice. The decreased level of Beclin-1 in APP/PS1/tau mice or APP/PS1/tau + shCon mice was reversed by *MCU* knockdown in hippocampal neurons. The level of P62 in APP/PS1/tau mice was higher than that in WT mice. The increased level of P62 in APP/PS1/tau mice or APP/PS1/tau + shCon mice was reversed by *MCU* knockdown in hippocampal neurons. $n = 3$ for each group. $^{*}P < 0.05$, $^{**}P < 0.01$. (G) Typical electron micrographs of mitochondria in the four groups. Swelling and cavitation of mitochondriain hippocampal neurons and broken mitochondrial cristae were observed in the APP/PS1/tau and APP/PS1/tau + shCon groups and were reduced in the APP/PS1/tau + shMCU group. (H) Histograms showed that the average volume of mitochondria was smaller in APP/PS1/tau mice than in WT mice; the average volume of mitochondria in APP/PS1/tau mice or APP/PS1/tau + shCon mice was increased by *MCU* knockdown in hippocampal neurons. (I) Histograms showed that mitochondria number was higher in APP/PS1/tau mice than in WT mice; mitochondria number in APP/PS1/tau mice or APP/PS1/tau + shCon mice was decreased by *MCU* knockdown in hippocampal neurons. $n = 6$ for each group. $^{*}P < 0.05$, $^{**}P < 0.01$, $^{***}P < 0.001$.

calcium dysregulation hypothesis of AD states that disruption to neuronal calcium signaling balance underlies not only amyloid plaque deposition and tau hyperphosphorylation [21] but also a series of molecular changes within the neuron that cause neuronal death [22]. Neurons are extremely sensitive to mCa^{2+} overload [23,24]. Transport of calcium into the matrix across the inner mitochondrial membrane is mainly accomplished by MCU, with high calcium selectivity [25]. Therefore, MCU mediating mCa^{2+} uptake plays a key role in mitochondrial calcium homeostasis in neurons. It was reported that MCU overexpression could clearly cause neuronal death [26]. Thus, downregulating the activity of MCU might represent a promising therapy for the prevention and treatment of AD [16,27]. It was found that reducing mCa^{2+} uptake can improve neuronal dysfunction and mitochondrial morphology in presenilin mutants [28]. Decreasing mCa^{2+} influx in presenilin mutants could rescue the defects in proteostasis [29] and autophagy [30]. In contrast, increased mCa^{2+} level was associated with plaque deposition and neuronal death in a transgenic mouse model of cerebral β-amyloidosis, which was prevented by blocking MCU [25]. A recent report showed that intracerebroventricular (ICV) injection of RU360, an MCU blocker, reduced cognitive defects induced by amyloid beta protein (Aβ). In the present study, we showed that the expression level of MCU in the hippocampus of APP/PS1/tau transgenic mice was much higher than that in the hippocampus of control mice [31]. Next, we prepared APP/PS1/tau mice with stable *MCU* knockdown in hippocampal neurons and observed that *MCU* knockdown in hippocampal neurons reversed the impairments in working memory (the short-term memory for the information changed in every trial) and reference memory (the long-term memory for the information remained constant over repeated trials) in APP/PS1/tau mice. Our findings demonstrate that *MCU* knockdown in hippocampal neurons could be beneficial for improving memory performance in AD, in agreement with previous work.

Synapses are fundamental elements of information transfer and memory storage in the brain [32]. Various synaptic proteins expressed in the presynaptic terminals and in the postsynaptic density are involved in the regulation of synaptic function [33]. Multiple studies have shown that defective synaptic transmission or loss of synapses in the hippocampus strongly correlates with memory decline in AD [34,35]. In this study, we measured the synaptic protein levels of PSD95 and SYP. PSD95, a major scaffolding protein in postsynaptic density (PSD), is a potent regulator of synaptic strength and plasticity [18]. SYP, which is enriched in presynaptic nerve terminals, is regarded as an accurate index of neuronal synaptic densities [18]. Western blot analysis results clearly demonstrated a significant reduction in the expression levels of PSD95 and SYP in the hippocampus of APP/PS1/tau mice, which were upregulated by *MCU* knockdown in hippocampal neurons. In addition, the numbers of synapses and dendritic spines were greatly reduced in APP/PS1/tau mice and were increased by *MCU* knockdown in hippocampal neurons. These results can explain the improvement in memory performance of APP/PS1/tau mice through *MCU* knockdown in hippocampal neurons.

Neuroinflammation has a significant influence on the progression of AD [36]. Microglia play a major role in mediating the inflammatory response in the AD brain [37]; however, recent evidence has suggested that astrocytes also play a key role in the neuroinflammatory response of AD [38,39]. Astrocytes are essential components of synapses, which are responsible for bidirectional communication between pre- and postsynaptic neurons [40]. Marked by the increase in glial fibrillary acidic protein (GFAP), astrogliosis could be observed in postmortem tissues from AD patients and mouse models. Moreover, the degree of astrogliosis is correlated with cognitive decline. Activated astrocytes secrete proinflammatory cytokines that are upregulated in human AD brain samples and in transgenic mouse models of AD, notably IL-1β and TNF-α [41]. IL-1β, one of the first cytokines secreted in response to injury, is an important mediator of the inflammatory response as well as cell proliferation, differentiation and apoptosis [42]. TNF-α, a cytokine involved in inducing acute-phase inflammation, is elevated in AD serum, CSF and cortex. Recently, a study showed that mitochondrial dysfunction triggered the inflammatory response [43]. Thus, decreasing the high expression of MCU in the hippocampus of AD patients might reduce the inflammatory response in AD [44]. In our study, *MCU* knockdown in hippocampal neurons resulted in a significant decrease in the neuroinflammatory response induced by astrogliosis and levels of IL-1β and TNF-α in APP/PS1/tau mice. This finding illustrates that *MCU* knockdown in hippocampal neurons has anti-inflammatory effects, perhaps supporting the improvement of memory performance in APP/PS1/tau mice.

Recent studies have revealed that autophagy plays a key role in AD [45]. Autophagy is essential for cell survival, and autophagy dysfunction is associated with neurodegenerative diseases [46]. Mitophagy is a mechanism of selective removal of damaged mitochondria and timely removal of damaged mitochondria. It plays an important role in maintaining the normal physiological function of cells [47]. Before memory defects occur in both AD patients and animal models, the accumulation of dysfunctional mitochondria is a common feature, illustrating that mitophagy is impaired in AD [48]. It was reported that impaired mitophagy could trigger accumulation of amyloid β (Aβ) and hyperphosphorylation of tau protein by aggravating oxidative damage, resulting in synaptic dysfunction and memory impairment [49]. Regulation of mitophagy might provide a new method for the treatment of AD [50]. At present, five main mitophagy pathways have been reported in mammals, and the PINK1/Parkin pathway is the focus of current research [51]. Phosphatase and tensin homologue (PTEN)-induced putative kinase 1 (PINK1) is a serine/threonine protein kinase located in the outer membrane of mitochondria. Phosphorylation of PINK1 activates Parkin, and Parkin translocates from the cytoplasm to mitochondria, promoting ubiquitination of mitochondrial outer membrane proteins and activation of the ubiquitin–proteasome system (UPS), mediating mitochondrial autophagy [52]. Increasing the expressions of PINK1 and Parkin could promote the clearance of damaged mitochondria in AD mice, alleviating synaptic loss and cognitive impairments [53,54]. Increasing the expression of PINK1 by gene therapy could lessen the Aβ plaque load in AD mice [55]. Alleviating the accumulation of Aβ and decreasing the level of Aβ can be achieved by increasing the expression of Parkin [56]. Cells overexpressing Parkin treated with Aβ had lower ROS production [57]. The learning and memory of $Aβ_{1-42}$-injected AD rats was improved by upregulating PINK1-Parkin-mediated mitophagy [58]. A study showed that activation of mitophagy reduced the level of pathological tau protein, while PINK1 knockdown abolished this effect [49]. PINK1 overexpression significantly alleviated the deposition of pathological tau, neuron loss, synaptic damage and

cognitive impairments in mice [59]. In addition, amyloid and hyperphosphorylation of tau protein further aggravates the damage of mitophagy, which results in a vicious cycle, promoting the process of AD [60]. Our results show that *MCU* knockdown in hippocampal neurons can upregulate the PINK1/Parkin pathway, increase the level of Beclin-1 and decrease the level of P62, playing a vital role in the PINK1/Parkin pathway [56], which could explain how *MCU* knockdown in hippocampal neurons reverses memory performance decline in APP/PS1/tau mice. The study of Parkinson's disease (PD) suggested that modulation of MCU-mediated mitochondrial calcium homeostasis is a possible neuroprotective strategy in PINK1 mutant PD, which is in agreement with our results [61]. Furthermore, due to abnormal mitochondrial division, the average volume of mitochondria was smaller and the number of mitochondria was higher in APP/PS1/tau mice than in WT mice, reflecting mitophagy dysfunction in AD, which was relieved by *MCU* knockdown in hippocampal neurons.

In summary, our findings demonstrated that *MCU* knockdown in hippocampal neurons could improve the memory performance of APP/PS1/tau mice by upregulating the levels of the synaptic markers PSD95 and SYP and increasing the numbers of synapses and dendritic spines; attenuating the neuroinflammatory response induced by astrogliosis and decreasing the levels of the proinflammatory cytokines IL-1β and TNF-α; improving the PINK1-Parkin mitophagy signaling pathway; increasing the level of Beclin-1; decreasing the level of P62; and recovering the average volume and number of mitochondria. These observations suggest that MCU inhibition may be a potential strategy for the treatment of AD.

Funding

This work was supported by the grants from the National Natural Science Foundation of China (Nos. 31600865, 82171428, and 82271484), the Four "Batches" Innovation Project of Invigorating Medical through Science and Technology of Shanxi Province (No. 2021XM33), the Open Fund from Key Laboratory of Cellular Physiology (Shanxi Medical University), the Ministry of Education, China (No. KLMEC/SXMU-202013), the Shanxi "1331 Project" Key Subjects Construction (No. 1331KSC), and the Research Project supported by Shanxi Scholarship Council of China (Nos. 2020-083, and 2022-115).

Conflict of Interest

The authors declare that they have no conflict of interest.

References

1. Liu Y, Chu JMT, Yan T, Zhang Y, Chen Y, Chang RCC, Wong GTC. Short-term resistance exercise inhibits neuroinflammation and attenuates neuropathological changes in 3xTg Alzheimer's disease mice. *J Neuroinflammation* 2020, 17: 4
2. Jia J, Wei C, Chen S, Li F, Tang Y, Qin W, Zhao L, *et al.* The cost of Alzheimer's disease in China and re-estimation of costs worldwide. *Alzheimers Dement* 2018, 14: 483–491
3. Briggs R, Kennelly SP, O'Neill D. Drug treatments in Alzheimer's disease. *Clin Med* 2016, 16: 247–253
4. Volloch V, Olsen BR, Rits S. AD "statin": Alzheimer's disorder is a "fast" disease preventable by therapeutic intervention initiated even late in life and reversible at the early stages. *Ann Integr Mol Med* 2019, 2: 75
5. Mancini G, Dias C, Lourenço CF, Laranjinha J, de Bem A, Ledo A. A high fat/cholesterol diet recapitulates some Alzheimer's disease-like features in mice: focus on hippocampal mitochondrial dysfunction. *J Alzheimer Dis* 2021, 82: 1619–1633
6. Yao J, Irwin RW, Zhao L, Nilsen J, Hamilton RT, Brinton RD. Mitochondrial bioenergetic deficit precedes Alzheimer's pathology in female mouse model of Alzheimer's disease. *Proc Natl Acad Sci USA* 2009, 106: 14670–14675
7. Oliver DMA, Reddy PH. Molecular basis of Alzheimer's disease: focus on mitochondria. *J Alzheimer Dis* 2019, 72: S95–S116
8. Picone P, Nuzzo D, Caruana L, Scafidi V, Di Carlo M. Mitochondrial dysfunction: different routes to Alzheimer's disease therapy. *Oxid Med Cell Longev* 2014, 2014: 1–11
9. Aman Y, Ryan B, Torsetnes SB, Knapskog AB, Watne LO, McEwan WA, Fang EF. Enhancing mitophagy as a therapeutic approach for neurodegenerative diseases. *Int Rev Neurobiol* 2020, 155: 169-202.
10. Ren T, Zhang H, Wang J, Zhu J, Jin M, Wu Y, Guo X, *et al.* MCU-dependent mitochondrial Ca2 + inhibits NAD + /SIRT3/SOD2 pathway to promote ROS production and metastasis of HCC cells. *Oncogene* 2017, 36: 5897–5909
11. Calvo-Rodriguez M, Bacskai BJ. Mitochondria and calcium in Alzheimer's disease: from cell signaling to neuronal cell death. *Trends Neuroscis* 2021, 44: 136–151
12. Bisbach CM, Hutto RA, Poria D, Cleghorn WM, Abbas F, Vinberg F, Kefalov VJ, *et al.* Mitochondrial calcium uniporter (MCU) deficiency reveals an alternate path for Ca2 + uptake in photoreceptor mitochondria. *Sci Rep* 2020, 10: 16041
13. Baughman JM, Perocchi F, Girgis HS, Plovanich M, Belcher-Timme CA, Sancak Y, Bao XR, *et al.* Integrative genomics identifies MCU as an essential component of the mitochondrial calcium uniporter. *Nature* 2011, 476: 341–345
14. Davey DA. Alzheimer's disease, dementia, mild cognitive impairment and the menopause: a 'window of opportunity' ? *Womens Health (Lond Engl)* 2013, 9: 279–290
15. Harrington JL, Murphy E. The mitochondrial calcium uniporter: mice can live and die without it. *J Mol Cell Cardiol* 2015, 78: 46–53
16. Venugopal A, Iyer M, Balasubramanian V, Vellingiri B. Mitochondrial calcium uniporter as a potential therapeutic strategy for Alzheimer's disease. *Acta Neuropsychiatr* 2020, 32: 65–71
17. Song AQ, Gao B, Fan JJ, Zhu YJ, Zhou J, Wang YL, Xu LZ, *et al.* NLRP1 inflammasome contributes to chronic stress-induced depressive-like behaviors in mice. *J Neuroinflammation* 2020, 17: 178
18. Li T, Jiao JJ, Su Q, Hölscher C, Zhang J, Yan XD, Zhao HM, *et al.* A GLP-1/GIP/Gcg receptor triagonist improves memory behavior, as well as synaptic transmission, neuronal excitability and Ca^{2+} homeostasis in 3xTg-AD mice. *Neuropharmacology* 2020, 170: 108042
19. Cai HY, Yang D, Qiao J, Yang JT, Wang ZJ, Wu MN, Qi JS, *et al.* A GLP-1/GIP dual receptor agonist DA4-JC effectively attenuates cognitive impairment and pathology in the APP/PS1/Tau model of alzheimer's disease. *J Alzheimer Dis* 2021, 83: 799–818
20. Tong BCK, Lee CSK, Cheng WH, Lai KO, Kevin Foskett J, Cheung KH. Familial Alzheimer's disease–associated presenilin 1 mutants promote γ-secretase cleavage of STIM1 to impair store-operated Ca^{2+} entry. *Sci Signal* 2016, 9: ra89
21. Zhao Y, Sivaji S, Chiang MC, Ali H, Zukowski M, Ali S, Kennedy B, *et al.* Amyloid beta peptides block new synapse assembly by nogo receptor-mediated inhibition of t-type calcium channels. *Neuron* 2017, 96: 355–372.e6
22. Zhang I, Hu H. Store-operated calcium channels in physiological and pathological states of the nervous system. *Front Cell Neurosci* 2020, 14:

600758
23. Jadiya P, Garbincius JF, Elrod JW. Reappraisal of metabolic dysfunction in neurodegeneration: focus on mitochondrial function and calcium signaling. *Acta Neuropathol Commun* 2021, 9: 124
24. Wu AJ, Tong BCK, Huang AS, Li M, Cheung KH. Mitochondrial calcium signaling as a therapeutic target for Alzheimer's disease. *Curr Alzheimer Res* 2020, 17: 329–343
25. Calvo-Rodriguez M, Hou SS, Snyder AC, Kharitonova EK, Russ AN, Das S, Fan Z, *et al.* Increased mitochondrial calcium levels associated with neuronal death in a mouse model of Alzheimer's disease. *Nat Commun* 2020, 11: 2146
26. Granatiero V, Pacifici M, Raffaello A, De Stefani D, Rizzuto R. Overexpression of mitochondrial calcium uniporter causes neuronal death. *Oxid Med Cell Longev* 2019, 2019: 1–15
27. Esteras N, Abramov AY. Mitochondrial calcium deregulation in the mechanism of beta-amyloid and tau pathology. *Cells* 2020, 9: 2135
28. Sarasija S, Laboy JT, Ashkavand Z, Bonner J, Tang Y, Norman KR. Presenilin mutations deregulate mitochondrial Ca^{2+} homeostasis and metabolic activity causing neurodegeneration in Caenorhabditis elegans. *eLife* 2018, 7: 33052
29. Ashkavand Z, Sarasija S, Ryan KC, Laboy JT, Norman KR. Corrupted ER-mitochondrial calcium homeostasis promotes the collapse of proteostasis. *Aging Cell* 2020, 19: e13065
30. Ryan KC, Ashkavand Z, Sarasija S, Laboy JT, Samarakoon R, Norman KR. Increased mitochondrial calcium uptake and concomitant mitochondrial activity by presenilin loss promotes mTORC1 signaling to drive neurodegeneration. *Aging Cell* 2021, 20: e13472
31. Nikseresht Z, Ahangar N, Badrikoohi M, Babaei P. Synergistic enhancing-memory effect of D-serine and RU360, a mitochondrial calcium uniporter blocker in rat model of Alzheimer's disease. *Behav Brain Res* 2021, 409: 113307
32. Zwamborn RAJ, Snijders C, An N, Thomson A, Rutten BPF, and de Nijs L. Wnt signaling in the hippocampus in relation to neurogenesis, neuroplasticity, stress and epigenetics. *Prog Mol Biol Transl Sci* 2018, 158: 129-157
33. Zoidl G, Petrasch-Parwez E, Ray A, Meier C, Bunse S, Habbes HW, Dahl G, *et al.* Localization of the pannexin1 protein at postsynaptic sites in the cerebral cortex and hippocampus. *Neuroscience* 2007, 146: 9–16
34. Zussy C, Loustalot F, Junyent F, Gardoni F, Bories C, Valero J, Desarménien MG, *et al.* Coxsackievirus adenovirus receptor loss impairs adult neurogenesis, synapse content, and hippocampus plasticity. *J Neurosci* 2016, 36: 9558–9571
35. Scheff SW, Price DA, Ansari MA, Roberts KN, Schmitt FA, Ikonomovic MD, Mufson EJ. Synaptic change in the posterior cingulate gyrus in the progression of alzheimer's disease. *J Alzheimer Dis* 2015, 43: 1073–1090
36. Zuo Z, Qi F, Yang J, Wang X, Wu Y, Wen Y, Yuan Q, *et al.* Immunization with Bacillus Calmette-Guérin (BCG) alleviates neuroinflammation and cognitive deficits in APP/PS1 mice via the recruitment of inflammation-resolving monocytes to the brain. *NeuroBiol Dis* 2017, 101: 27–39
37. Zuroff L, Daley D, Black KL, Koronyo-Hamaoui M. Clearance of cerebral Aβ in Alzheimer's disease: reassessing the role of microglia and monocytes. *Cell Mol Life Sci* 2017, 74: 2167–2201
38. Thangavel R, Stolmeier D, Yang X, Anantharam P, Zaheer A. Expression of glia maturation factor in neuropathological lesions of Alzheimer's disease. *NeuroPathol Appl NeuroBiol* 2012, 38: 572–581
39. Zhang P, Li YX, Zhang ZZ, Yang Y, Rao JX, Xia L, Li XY, *et al.* Astroglial mechanisms underlying chronic insomnia disorder: a clinical study. *Nat Sci Sleep* 2020, 12: 693–704
40. Bonansco C, Couve A, Perea G, Ferradas CÁ, Roncagliolo M, Fuenzalida M. Glutamate released spontaneously from astrocytes sets the threshold for synaptic plasticity. *Eur J Neurosci* 2011, 33: 1483–1492
41. Zumkehr J, Rodriguez-Ortiz CJ, Medeiros R, Kitazawa M. Inflammatory cytokine, IL-1β, regulates glial glutamate transporter via microRNA-181a in vitro. *J Alzheimer Dis* 2018, 63: 965–975
42. Ng A, Tam WW, Zhang MW, Ho CS, Husain SF, McIntyre RS, Ho RC. IL-1β, IL-6, TNF-α and CRP in elderly patients with depression or Alzheimer's disease: systematic review and meta-analysis. *Sci Rep* 2018, 8: 12050
43. Joshi AU, Minhas PS, Liddelow SA, Haileselassie B, Andreasson KI, Dorn Ii GW, Mochly-Rosen D. Fragmented mitochondria released from microglia trigger A1 astrocytic response and propagate inflammatory neurodegeneration. *Nat Neurosci* 2019, 22: 1635–1648
44. Rose J, Brian C, Woods J, Pappa A, Panayiotidis MI, Powers R, Franco R. Mitochondrial dysfunction in glial cells: implications for neuronal homeostasis and survival. *Toxicology* 2017, 391: 109–115
45. Li Q, Liu Y, Sun M. Autophagy and Alzheimer's disease. *Cell Mol Neurobiol* 2017, 37: 377–388
46. Pierzynowska K, Gaffke L, Cyske Z, Puchalski M, Rintz E, Bartkowski M, Osiadły M, *et al.* Autophagy stimulation as a promising approach in treatment of neurodegenerative diseases. *Metab Brain Dis* 2018, 33: 989–1008
47. Shefa U, Jeong NY, Song IO, Chung HJ, Kim D, Jung J, Huh Y. Mitophagy links oxidative stress conditions and neurodegenerative diseases. *Neural Regen Res* 2019, 14: 749–756
48. Manczak M, Calkins MJ, Reddy PH. Impaired mitochondrial dynamics and abnormal interaction of amyloid beta with mitochondrial protein Drp1 in neurons from patients with Alzheimer's disease: implications for neuronal damage. *Hum Mol Genet* 2011, 20: 2495–2509
49. Fang EF, Hou Y, Palikaras K, Adriaanse BA, Kerr JS, Yang B, Lautrup S, *et al.* Mitophagy inhibits amyloid-β and tau pathology and reverses cognitive deficits in models of Alzheimer's disease. *Nat Neurosci* 2019, 22: 401–412
50. Lou G, Palikaras K, Lautrup S, Scheibye-Knudsen M, Tavernarakis N, Fang EF. Mitophagy and neuroprotection. *Trends Mol Med* 2020, 26: 8–20
51. Fivenson EM, Lautrup S, Sun N, Scheibye-Knudsen M, Stevnsner T, Nilsen H, Bohr VA, *et al.* Mitophagy in neurodegeneration and aging. *Neurochem Int* 2017, 109: 202–209
52. Wang P, Wang L, Lu J, Hu Y, Wang Q, Li Z, Cai S, *et al.* SESN2 protects against doxorubicin-induced cardiomyopathy via rescuing mitophagy and improving mitochondrial function. *J Mol Cell Cardiol* 2019, 133: 125–137
53. Du F, Yu Q, Yan S, Hu G, Lue LF, Walker DG, Wu L, *et al.* PINK1 signalling rescues amyloid pathology and mitochondrial dysfunction in Alzheimer's disease. *Brain* 2017, 140: 3233–3251
54. Ye X, Sun X, Starovoytov V, Cai Q. Parkin-mediated mitophagy in mutant hAPP neurons and Alzheimer's disease patient brains. *Hum Mol Genet* 2015, 24: 2938–2951
55. Quinn PMJ, Moreira PI, Ambrósio AF, Alves CH. PINK1/PARKIN signalling in neurodegeneration and neuroinflammation. *Acta Neuropathol Commun* 2020, 8: 189
56. Yang T, Zhao X, Zhang Y, Xie J, Zhou A. 6‴-Feruloylspinosin alleviated beta-amyloid induced toxicity by promoting mitophagy in Caenorhabditis elegans (GMC101) and PC12 cells. *Sci Total Environ* 2020, 715: 136953
57. Wang H, Zhang T, Ge X, Chen J, Zhao Y, Fu J. Parkin overexpression attenuates Aβ-induced mitochondrial dysfunction in HEK293 cells by restoring impaired mitophagy. *Life Sci* 2020, 244: 117322
58. Han Y, Wang N, Kang J, Fang Y. β-Asarone improves learning and memory in Aβ1-42-induced Alzheimer's disease rats by regulating PINK1-Parkin-mediated mitophagy. *Metab Brain Dis* 2020, 35: 1109–1117
59. Jiang XJ, Wu YQ, Ma R, Chang YM, Li LL, Zhu JH, Liu GP, *et al.* PINK1 alleviates cognitive impairments via attenuating pathological tau aggrega-

tion in a mouse model of tauopathy. *Front Cell Dev Biol* 2021, 9: 736267

60. Xu S, Yang P, Qian K, Li Y, Guo Q, Wang P, Meng R, ***et al.*** Modulating autophagic flux via ROS-responsive targeted micelles to restore neuronal proteostasis in Alzheimer's disease. *Bioactive Mater* 2022, 11: 300–316
61. Soman SK, Bazała M, Keatinge M, Bandmann O, Kuznicki J. Restriction of mitochondrial calcium overload by *mcu* inactivation renders neuroprotective effect in zebrafish models of Parkinson's disease. *Biol Open* 2019, 8: bio044347